

**Supporting Information for**  
**Computational Studies of Electrochemical CO<sub>2</sub> Reduction on Subnanometer Transition**  
**Metal Clusters**

*Cong Liu, Haiying He, Peter Zapol and Larry A. Curtiss\**

Materials Science Division, Argonne National Laboratory, 9700 S Cass Ave. Lemont IL 60439  
USA

\*(L.A.C.) Email: curtiss@anl.gov Tel: +1(630)252-7380 Fax: +1(630)252-9555

**S1. Computational Details**

All the Gibbs free energies were calculated in gas phase at 298.15K, in which all the gaseous molecules (CO<sub>2</sub>, CO, H<sub>2</sub> and CH<sub>4</sub>) and all the metal cluster containing systems were calculated at 101325Pa, while the liquid phase molecules (H<sub>2</sub>O, HCOOH and CH<sub>3</sub>OH) were calculated under their corresponding vapor fugacity, which comes from their vapor-liquid equilibrium with water and corresponds to a liquid mole fraction of 0.01.

Table S1. Structures of tetra-atomic metal clusters calculated by this work and previous studies

Cluster	This Work			Previous Studies		
	Ground-state Multiplicity	Geometry	Method	Ground-state Multiplicity	Geometry	Ref.
Fe <sub>4</sub>	9	Tetrahedral	PBE/DZP	-	Tetrahedral	1
Co <sub>4</sub>	11	Rhombus	PW91/DNP	11	Rhombus	2
Ni <sub>4</sub>	5	Tetrahedral	BP/[6s5p3d]	5	Tetrahedral	3
Cu <sub>4</sub>	3	Rhombus	PW91/DNP	-	Rhombus	4
Rh <sub>4</sub>	7	Tetrahedral	PW91	1	Tetrahedral	5
Pd <sub>4</sub>	3	Tetrahedral	MRSDCI and MRSDCI+Q	3	Tetrahedral	6
Ag <sub>4</sub>	1	Rhombus	PBE/ DZP	-	Rhombus	7
Ir <sub>4</sub>	9	Square-planar	BP/[8s,7p,5d,3f]	9	Square-planar	8
Pt <sub>4</sub>	3	Tetrahedral	MRSDCI and MRSDCI+Q	3	Tetrahedral	6
Au <sub>4</sub>	1	Triangle C <sub>2v</sub>	B3LYP/LANL2DZ	-	Triangle C <sub>2v</sub>	9

Various computational studies have been carried out to predict the ground state electronic structures of tetra-atomic metal clusters<sup>1-9</sup>. In this study, ten tetra-atomic clusters (Fe<sub>4</sub>, Co<sub>4</sub>, Ni<sub>4</sub>, Cu<sub>4</sub>, Ir<sub>4</sub>, Pd<sub>4</sub>, Ag<sub>4</sub>, Rh<sub>4</sub>, Pt<sub>4</sub> and Au<sub>4</sub>) were calculated using the B3LYP functional. The 6-31G\* basis set was applied to all the main group elements. An improved 6-31G\* basis set, m6-31G\*, was utilized for all the 3d metals, and the LANL2DZ basis set was used for all the 4d and 5d metals. To assess the reliability of the B3LYP functional, the B3LYP results were compared with previous computational studies, shown in Table S1. In general, the structures of the clusters calculated in the present work have good agreement with previous studies<sup>1-9</sup>.

Table S2. Adsorption free energies of CO<sub>2</sub> to tetra-atomic metal clusters calculated at B3LYP (without empirical corrections to CO<sub>2</sub> molecule), M06, PBE0 and CCSD(T) levels of theory (eV)

Cluster	$\Delta G$ B3LYP	$\Delta G$ M06	$\Delta G$ PBE0	$\Delta G$ CCSD(T)
Fe <sub>4</sub>	-0.73	-3.04	-1.14	
Co <sub>4</sub>	-0.56	-0.72	-0.68	
Ni <sub>4</sub>	-1.05	-1.36	-1.50	
Cu <sub>4</sub>	0.09	0.11	-0.07	0.13
Rh <sub>4</sub>	-0.05	-0.11	0.14	
Pd <sub>4</sub>	0.09	0.02	0.07	
Ag <sub>4</sub>	0.12	0.07	0.11	0.05
Ir <sub>4</sub>	0.20	0.12	0.17	
Pt <sub>4</sub>	0.24	0.28	-0.10	
Au <sub>4</sub>	0.10	0.08	0.07	-0.01

In addition to B3LYP, the adsorption free energies of CO<sub>2</sub> to the ten clusters were calculated using the M06, PBE0 and CCSD(T) methods (only Cu, Ag and Au clusters were calculated using CCSD(T) method), based on the B3LYP geometries and thermal correction. As shown in Table S2, the more negative the adsorption free energies are, the stronger CO<sub>2</sub> binds to the cluster. The B3LYP binding energies showed the same signs (positive or negative values) with the M06 values, while PBE0 values showed opposite signs with the other two methods for the Cu<sub>4</sub>, Rh<sub>4</sub> and Pt<sub>4</sub> systems. Generally, all three DFT functionals suggested that Fe<sub>4</sub>, Co<sub>4</sub> and Ni<sub>4</sub> have much stronger binding with CO<sub>2</sub>, compared to the other metal clusters. Compared to the CCSD(T) results for Cu, Ag and Au systems, M06 gave the smallest deviation (MAD=0.04eV) among the three functionals. However, the M06 energy of Fe system is extremely low (-3.04eV), which

does not agree with the other two functionals. This implies the M06 value of Fe system may not be reliable. On the other hand, the B3LYP binding energies showed smaller deviations (MAD=0.07eV) than the PBE0 values (MAD=0.11eV) compared to the CCSD(T) results, and the adsorption free energies of Fe<sub>4</sub>, Co<sub>4</sub>, Ni<sub>4</sub> and Cu<sub>4</sub> showed the same trend (Ni < Fe < Co < Cu) with both B3LYP and PBE0 functionals. Since this work is focused on the comparisons and tendency of the metal clusters for the electrocatalysis of CO<sub>2</sub>, the B3LYP functional was selected to study the reaction energetics based on its reliability and acceptable accuracy.

Table S3. Atomization energies of selected molecules and radicals (eV)

	Expt. <sup>10</sup>	B3LYP/6-31G*	Error/Empirical correction
H <sub>2</sub>	4.488	4.484	-0.004
H <sub>2</sub> O	9.509	8.887	-0.622
CO	11.109	10.816	-0.293
CO <sub>2</sub>	16.560	16.375	-0.184
CH <sub>4</sub>	17.019	17.028	0.009
CH <sub>3</sub> OH	20.848	20.542	-0.306
HCOOH	20.835	20.501	-0.334
COOH	17.128	16.240	-0.887
OH	4.393	4.197	-0.195
HCO	11.721	11.698	-0.023
H <sub>2</sub> CO	15.493	15.406	-0.087
H <sub>3</sub> CO	16.367	16.521	0.154
C <sub>2</sub> H <sub>4</sub>	23.064	22.926	-0.138

Table S4. Reaction enthalpies of selected reactions (eV) ( $\Delta H_{\text{ref}}$  values were calculated from the enthalpies of formation<sup>10</sup>)

	Reaction	$\Delta H_{\text{ref}}$	B3LYP/6-31G*	Error	Error after correction
1	CO <sub>2</sub> + H <sub>2</sub> → CO + H <sub>2</sub> O	0.43	1.16	0.73	0.00
2	4 H <sub>2</sub> + CO <sub>2</sub> → CH <sub>4</sub> + 2 H <sub>2</sub> O	-1.71	-0.63	1.08	0.04
3	3 H <sub>2</sub> + CO → CH <sub>4</sub> + H <sub>2</sub> O	-2.14	-1.80	0.34	0.03
4	CO <sub>2</sub> + H <sub>2</sub> → HCOOH	0.15	0.28	0.13	-0.02
5	CO + H <sub>2</sub> O → HCOOH	-0.27	-0.88	-0.61	-0.03
6	3 H <sub>2</sub> + CO <sub>2</sub> → CH <sub>3</sub> OH + H <sub>2</sub> O	-0.55	0.25	0.80	0.07
7	2 H <sub>2</sub> + CO → CH <sub>3</sub> OH	-0.98	-0.91	0.07	0.06
8	3 H <sub>2</sub> + CO <sub>2</sub> → 1/2 C <sub>2</sub> H <sub>4</sub> + 2 H <sub>2</sub> O	-0.66	0.48	1.14	0.03
9	2 H <sub>2</sub> + CO → 1/2 C <sub>2</sub> H <sub>4</sub> + H <sub>2</sub> O	-1.09	-0.68	0.41	0.02

Since the B3LYP/6-31G\* method is used to calculate the reaction energies we have carried out calculations of the B3LYP/6-31G\* atomization energies of small molecules and radicals related to the present work and compared with experiment. The results are given in Table S3. The errors of the atomization energies of H<sub>2</sub>O, CO, CH<sub>3</sub>OH, HCOOH and COOH are significant, while those of the other systems are less than 0.2 eV. These errors may affect the energies of certain reactions, such as the water-gas shift reaction. Therefore, the reaction enthalpies of 9 reactions were analyzed, and corrections were added to the total energies for each molecule based on the errors of the atomization energies against experiment (Table S3). Shown in Table S4, before correction, B3LYP/6-31G\* yields large errors for some of the analyzed reactions, especially reactions 2 and 8. The small errors shown for reactions 3 and 7 are mainly due to error cancellation. After the empirical corrections were added to each molecule, the errors were reduced to no more than 0.07 eV. In the present work, corresponding empirical corrections (Table S3) were added to the total energies of related small molecules and radicals calculated by B3LYP/6-31G\* to obtain more accurate reaction free energies. For the PBE/plane wave calculations, the same corrections as that Peterson et al.<sup>11</sup> suggested for PBE calculations were used.

## S2. Reaction Network of the Electrochemical Reduction of CO<sub>2</sub> to Fuels

A reaction network containing 38 intermediates was studied for the electrochemical reduction of CO<sub>2</sub> to HCOOH, CO, CH<sub>4</sub>, CH<sub>3</sub>OH and C<sub>2</sub>H<sub>4</sub> (Figure S1). In general, the reaction pathways in the network are initiated by three major reactions:



Eqn. 1 is the chemisorption of CO<sub>2</sub>, Eqn. 2 and 3 are the electrochemical adsorption of CO<sub>2</sub> with the proton transferred to an oxygen atom and the carbon atom, respectively. The reaction free energies of all elementary steps were calculated. The highlighted reaction pathway in Figure S1 was identified to be the thermodynamically most favorable pathway for all five considered clusters (Fe<sub>4</sub>, Co<sub>4</sub>, Ni<sub>4</sub>, Cu<sub>4</sub> and Pt<sub>4</sub>). This pathway is initiated by Eqn. 2. On the other hand, the reaction pathways initiated by Eqn. 3 are not thermodynamically favorable. The reaction pathways gave either highly endergonic or highly exergonic reactions, engendering thermodynamic sinks. Thus this pathway was eliminated in the beginning. The CO<sub>2</sub>

chemisorption is endergonic for  $\text{Cu}_4$  and  $\text{Pt}_4$ , and the C-O cleavage barriers of  $\text{CO}_2$  are extremely high for these two metal clusters, therefore the pathways initiated by Eqn. 1 are not thermodynamically favorable for  $\text{Cu}_4$  and  $\text{Pt}_4$  clusters. However, chemisorption of  $\text{CO}_2$  and C-O cleavage of  $\text{CO}_2$  are spontaneous for  $\text{Fe}_4$ ,  $\text{Co}_4$  and  $\text{Ni}_4$  clusters, and the barriers of C-O cleavage are below 1 eV. Therefore, as in the main text, the thermodynamically most favorable pathway was presented for all five clusters, and the  $\text{CO}_2$  chemisorption initiated pathway was also considered for  $\text{Fe}_4$ ,  $\text{Co}_4$  and  $\text{Ni}_4$  clusters.

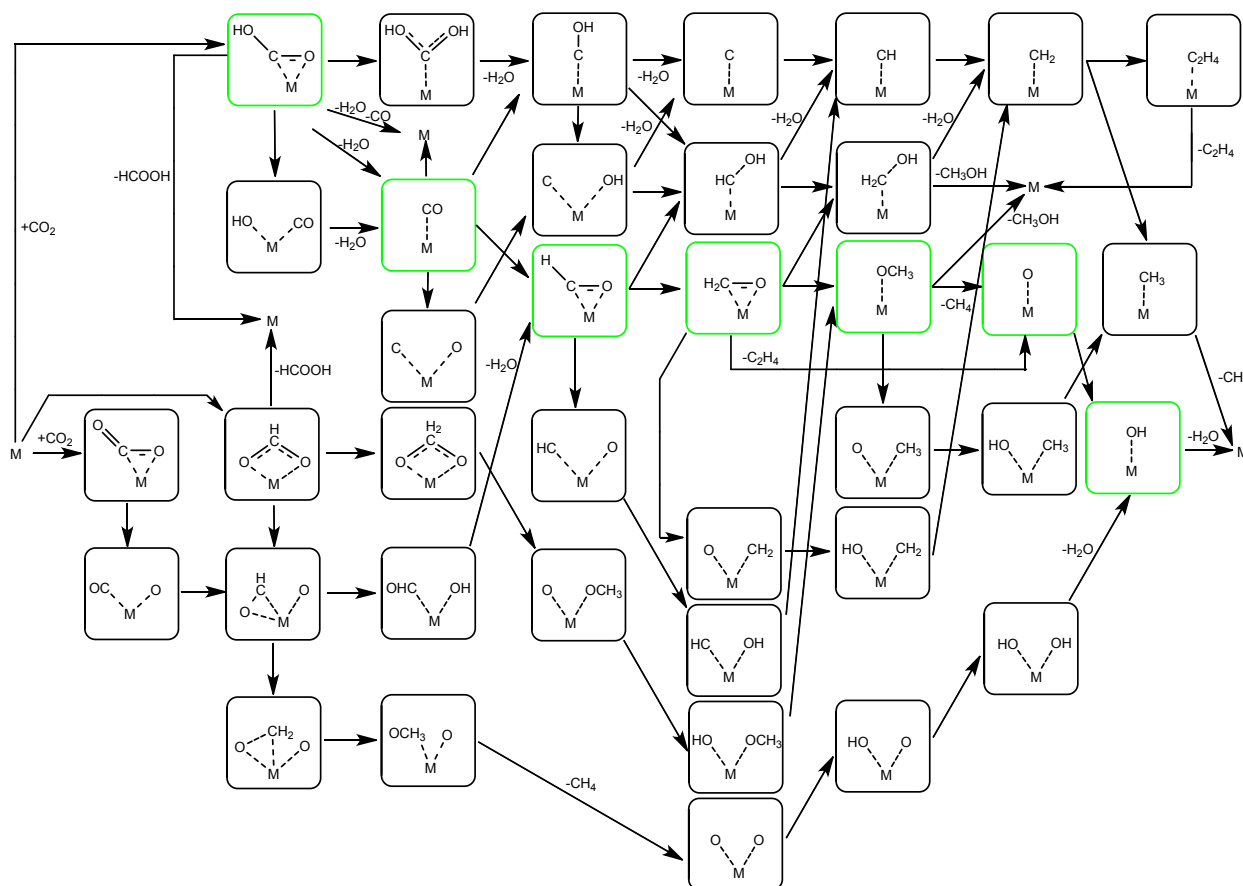


Figure S1. Reaction network of the electrochemical reduction of  $\text{CO}_2$  to fuels (M represents the tetra-atomic metal cluster)

### S3. Ground State Multiplicities and Relative Energies

All possible multiplicities of all species were taken into account. The ground state multiplicities and relative free energies of the species in the discussed pathways (pathways 1 and 2 in the main text) are listed in Table S3, where the index numbers correspond to the indices of intermediates in Figures 2-6 in the main text. The energies of all the states relative to the initial state, \* + CO<sub>2</sub>, were calculated using Eqn. 4:

$$G_{rel} = G_{state} - G_{int} - nG_{(H^+ + e^-)} \quad (4),$$

where  $G_{state}$  is the calculated free energy of the considered state,  $G_{int}$  is the calculated free energy of the initial state,  $G_{(H^+ + e^-)}$  is the calculated free energy of a (proton + electron) pair, which equals to a half of the free energy of a H<sub>2</sub> molecule, and n is the total number of (proton + electron) pairs transferred to form the corresponding state from the initial state. For example, the relative free energy of state 4 (CHO\*) is calculated as:

$$G_{rel}(4) = G_{(CHO^*)} - (G_{(*)} + G_{(CO_2)}) - 3(1/2G_{(H_2)})$$

Table S3. Multiplicities and relative free energies of the states (eV)

Cluster		Fe <sub>4</sub>		Co <sub>4</sub>		Ni <sub>4</sub>		Cu <sub>4</sub>		Pt <sub>4</sub>	
Index	State	Spin State	Relative Free Energy	Spin State	Relative Free Energy	Spin State	Relative Free Energy	Spin State	Relative Free Energy	Spin State	Relative Free Energy
1	* + CO <sub>2</sub>	9	0	11	0	5	0	3	0	3	0
2	COOH*	8	0.008	10	-0.083	6	-0.668	2	0.498	4	0.221
3	CO* + H <sub>2</sub> O	9	-0.712	9	-0.772	7	-1.115	1	-0.447	3	-1.418
4	CHO*	8	-0.328	10	-0.02	6	-0.688	2	0.603	2	-0.098
5	CH <sub>2</sub> O*	9	-0.642	9	-0.3	5	-0.894	1	0.168	3	-0.074
6	CH <sub>3</sub> O*	8	-1.274	10	-0.957	6	-1.334	2	-0.264	2	0.053
7	O* + CH <sub>4</sub>	9	-2.482	11	-1.697	5	-2.078	1	-0.141	5	0.254
8	OH*	8	-2.055	10	-1.964	6	-2.341	2	-1.347	4	-1.088
9	* + H <sub>2</sub> O	9	-1.335	11	-1.335	5	-1.335	1	-1.335	3	-1.335
2b	CO <sub>2</sub> *	7	-0.549	9	-0.371	5	-0.865				
3b	TS-CO <sub>2</sub> *	7	0.071	11	0.507	7	0.008				
4b	CO* + O*	7	-2.051	11	-0.813	3	-1.797				
5b	CHO* + O*	8	-1.558	10	-1.044	6	-1.355				
6b	CH <sub>2</sub> O* + O*	7	-2.193	11	-1.018	5	-1.219				
7b	CH <sub>3</sub> O* + O*	8	-2.228	10	-2.018	2	-1.986				
8b	O* + O* + CH <sub>4</sub>	9	-3.240	11	-2.587	7	-2.520				
9b	OH* + O*	8	-3.928	10	-3.040	6	-2.454				
10b	OH* + OH*	9	-3.224	9	-2.999	3	-3.867				
11b	OH* + H <sub>2</sub> O	8	-2.054	10	-1.966	6	-2.338				

## S4. Cu<sub>4</sub> vs. Supported Cu<sub>4</sub>

Table S4. Bader Charge Distribution in Cu<sub>4</sub> Cluster in Different Cu materials

Atom	Cu1	Cu2	Cu3	Cu4	Cu <sub>4</sub> cluster
Cu <sub>4</sub>	-0.1436	0.1772	0.1099	-0.1435	0
Cu <sub>4</sub> /Graphene	-0.1481	0.0815	0.2992	-0.1492	0.0834
Cu <sub>4</sub> /Defective graphene	0.0177	0.4935	-0.0172	0.2377	0.7317

## References

1. S. Yuan, Y. Kong, F. Wen and F. Li, *J. Phys.: Condens. Matter*, 2007, 19, 466203.
2. W. F. Hu, H. K. Yuan, H. Chen, G. Z. Wang and G. L. Zhang, *Phys. Lett. A*, 2014, 378, 198-206.
3. P. St. Petkov, G. N. Vayssilov, S. Krüger and N. Rösch, *Phys. Chem. Chem. Phys.*, 2006, 8, 1282.
4. X.-J. Kuang, X.-Q. Wang and G.-B. Liu, *Journal of Chemical Sciences*, 2011, 123, 743-754.
5. T. Futschek, M. Marsman and J. Hafner, *J. Phys.: Condens. Matter*, 2005, 17, 5927-5963.
6. D. Dai and K. Balasubramanian, *J. Chem. Phys.*, 1995, 103, 648.
7. R. Fournier, *J. Chem. Phys.*, 2001, 115, 2165.
8. C. Bussai, S. Krüger, G. N. Vayssilov and N. Rösch, *Phys. Chem. Chem. Phys.*, 2005, 7, 2656.
9. G. Zanti and D. Peeters, *Theor. Chem. Acc.*, 2012, 132.
10. National Institute of Standards and Technology (U.S.), in *NIST standard reference database 69*, National Institute of Standards and Technology., Washington, D.C., June 2005 release. edn.
11. A. A. Peterson, F. Abild-Pedersen, F. Studt, J. Rossmeisl and J. K. Nørskov, *Energy Environ. Sci.*, 2010, 3, 1311.